Serinc2 deficiency causes susceptibility to sepsis-associated acute lung injury

Shuai Mao
Renmin Hospital of Wuhan University: Wuhan University Renmin Hospital
Jian Lv
Renmin Hospital of Wuhan University: Wuhan University Renmin Hospital
Meng Chen
Wuhan University Zhongnan Hospital
Ningning Guo
Wuhan University Renmin Hospital
Yu Fang
Renmin Hospital of Wuhan University: Wuhan University Renmin Hospital
Jingjing Tong
Central China Normal University
Xianghu He
Wuhan University Zhongnan Hospital
Gang Wu
Renmin Hospital of Wuhan University: Wuhan University Renmin Hospital
Zhihua Wang (wangzhihua@fuwaihospital.org)
Fuwai Hospital State Key Laboratory of Cardiovascular Disease https://orcid.org/0000-0002-1800-2384

Research

Keywords: serinc2, acute lung injury, sepsis, lipopolysaccharide, inflammation, apoptosis

Posted Date: September 21st, 2021

DOI: https://doi.org/10.21203/rs.3.rs-907860/v1

Abstract

Background

Severe sepsis and its subsequent complications cause high morbidity and mortality rates worldwide. Lung is one of the most vulnerable organs sensitive to sepsis-associated inflammatory storm, and usually develops into acute respiratory distress syndrome (ARDS)/acute lung injury (ALI). The pathogenesis of sepsis-associated ALI is accompanied by coordinated transmembrane signal transduction and subsequent programmed cell death; however, the underlying mechanism remains largely unclear.

Results

Here we find that the expression of serine incorporator 2 (Serinc2), a protein involved in phosphatidylserine synthesis and membrane incorporation, is upregulated in cecal ligation and puncture (CLP)-induced ALI. Furthermore, serinc2-knockout (KO) mouse line is generated by CRISPR-cas9 approach. Compared with wildtype mice, the Serinc2-KO mice exhibit exacerbated ALI-related pathologies after CLP. The expressions of pro-inflammatory factors, including IL1β, IL6, TNFα, and MCP1, are significantly enhanced by Serinc2 deficiency, concurrent with over-activation of STAT3, p38 and ERK pathways. Conversely, Serinc2 overexpression in RAW264.7 cells significantly suppresses the inflammatory responses induced by lipopolysaccharide (LPS). Serinc2 KO aggravates CLP-induced apoptosis as evidenced by increases in TUNEL-positive staining, Bax expression, and Caspase-3 cleavage and decreases in BCL-2 expression and Akt phosphorylation, whereas these changes are suppressed by Serinc2 overexpression in LPS-treated RAW264.7 cells. Moreover, administration of AKTin, an inhibitor of Akt, abolishes the protective effects of Serinc2 overexpression against inflammation and apoptosis.

Conclusions

Our findings demonstrate a protective role of Serinc2 in the lung through activating the Akt pathway, and provide novel insight into the pathogenesis of sepsis-induced ALI.

Introduction

Severe sepsis is a major healthcare problem that affects millions of patients globally each year [1]. It causes devastating clinical illnesses, particularly acute respiratory distress syndrome (ARDS)/acute lung injury (ALI) [2]. Sepsis-induced ALI is characterized by large numbers of neutrophils, macrophages and erythrocytes in the alveoli, hyaline membranes in alveolar cavity, interstitial and alveolar edema, and necrosis of pulmonary endothelium and epithelium cells [2]. These pathologies are consequences of hyperactive host inflammatory responses to pathogens as evidenced by excessive release of chemokines and cytokines, such as IL1, IL6, CXCL2, TNFα and MCP-1 [3–6].

Hyperactivation of the immune system during ALI triggers apoptosis of pulmonary vascular endothelial cells and alveolar epithelial cells, causing alveolar capillary barrier damage, fluid leakage and pulmonary hemorrhage [7–9]. In turn, the clearance of apoptotic cell corpse further enhances the inflammatory response, leading to lethal cytokine storm [10]. How the inflammation and apoptosis pathways are coordinated during the pathogenesis of ALI remains largely unknown.

Serine incorporator 2 (Serinc2; also known as tumor differentially expressed protein 2, TDE2) belongs to the highly conserved Serinc family (1–5), which are responsible for serine synthesis and membrane incorporation [11]. It was firstly identified as an oncogene in non-small cell lung cancer by Player et al. in 2003 [12]. Zeng et al. [13] also found a high enrichment of Serinc2 in lung adenocarcinoma that regulating tumor cell proliferation, migration and invasion through PI3K/AKT signaling pathway. However, the physiological function of Serinc2 in the lung remain unexplored.

Here we generate a Serinc2-knockout (KO) mouse line, and find that Serinc2-KO mice are vulnerable to cecal ligation and puncture (CLP)-induced ALI. Whereas Serinc2 deficiency exacerbates severe inflammation and apoptosis, Serinc2 overexpression in raw264.7 cells prevents lipopolysaccharide (LPS)-induced over-activation of inflammation and apoptosis through activating the Akt signaling pathway. Our findings reveal a previously unrecognized protective role of Serinc2 in the pathogenesis of ALI, and provide novel targets to treat infection-associated ALI in clinic.

Materials And Methods

Generation of Serinc2-knockout mouse

CRISPR/Cas9 technology was used to delete the Serinc2 gene in mouse by targeting exon 2–10 of the Serinc2 transcript (ENSMUST00000122374.7). Recombinant Cas9 protein and in vitro transcribed sgRNA were microinjected into the fertilized eggs of C57BL/6JGpt mice. Fertilized eggs were transplanted to obtain positive F0 mice which were confirmed by PCR and sequencing. A stable F1 generation mouse model was obtained by mating positive F0 generation mice with C57BL/6JGpt mice. Then we inter-crossed heterozygous females and males for to obtain the third generation homozygous Serinc2$^{-/-}$ mice for formal experiments.

Animal care

All animal experiments procedures were reviewed and approved by the Institutional Animal Care and Use Committee (IACUC) of Renmin Hospital of Wuhan University and performed in accordance with the guide for the care and use of laboratory animals published by National Institutes of Health, USA (8th edition). All mice were raised in a specific pathogen free environment (temperature, 24 ± 3°C; humidity, 55 ± 5%) with a 12-h light/12-h dark cycle and fed normal chow.

Cecal ligation and puncture (CLP) surgery

Serinc2$^{-/-}$ and wildtype (WT) C57BL/6J mice were randomly assigned into sham or CLP groups. CLP surgery was performed as previously described [14]. Mice were anaesthetized with 1% pentobarbital sodium (50mg/kg) by intraperitoneal (i.p.) injection. After anesthesia, mice were fixed on the operation table, the abdominal hair was removed first, and a 1 midline cm incision was made along the abdominal white line. Then open the abdominal cavity layer by layer and find the cecum. the cecum was tightly ligated with 3 / 0 silk thread at 1 cm from the end of the cecum, and punctured twice at 0.5 cm from the distal end with No.7 needle. Then gently squeeze to extrude a small amount of feces. After replacing the cecum in the abdomen, the abdomen was closed in two layers. Mice in sham group underwent the same procedure except their cecums were neither ligated nor punctured.

Assessment of lung endothelial cell permeability

Lung endothelial cell permeability was detected by measuring the accumulation of Evans blue in the lungs. Evans blue (EB) dye solution (20mg/kg) was injected into the tail vein 30min before mice was sacrificed. Then lung tissues were perfused with PBS and collected. And the collected lung tissue was homogenized in a 37 ℃ bath for 24 hours and centrifuged at 3000g for 30 minutes. The EB content was determined by measuring the absorbance of the supernatant at 620 nm and corrected for hemoglobin content at 740 nm in the microplate reader according to the standard of known EB content.

Hematoxylin and Eosin (H&E) staining

Mice was sacrificed 24h after CLP. The lung tissues from part of the right middle lobe of the lung were collected and fixed with 4% paraformaldehyde at 25 ℃ for 24 h. After fixation, the lung tissue was embedded in paraffin with a slice thickness of 5μm. H&E was stained with hematoxylin for 10 min and eosin for 3 min at 25℃. The degree of lung injury was graded using a histologic ALI scoring system based on histologic features, including neutrophils, hyaling membranes, proteinaceous debris, and alveolar septal thickening. All lung fields at ×20 magnification were examined for each sample. Assessment of histological lung injury was performed by scoring from 1 to 5, with 1 being the best (normal lung) and 5 being the worst (most severe ALI). Scoring was performed as follows: 1, normal; 2, focal (< 50% lung section) interstitial congestion and inflammatory cell infiltration; 3, diffuse (> 50% lung section) interstitial congestion and inflammatory cell infiltration; 4, focal (< 50% lung section) consolidation (combining into a solid mass without the alveoli structure) and inflammatory cell infiltration and 5, diffuse (> 50% lung section) consolidation and inflammatory cell infiltration [15, 16].

Cell culture and treatment

RAW264.7 cells was cultured in DMEM containing 10% fetal bovine serum (FBS; Gibco, USA) and incubated at 37℃ in a humidified atmosphere containing 5% CO_2. RAW264.7 cells were stimulated with LPS (sigma, USA) to induce cellular damage as an in vitro ALI model. Plasmid pcDNA3.1-Serinc2-3·flag (4μg) and negative control pcDNA3.1-EGFP(4μg) were transiently transfected into RAW264.7 cells using Lipofectamine 2000 (6μl, Invitrogen, USA). Then, the cells were subjected to 1μg/ml LPS with or without an AKT inhibitor, AKTin (1μM). The cells were collected and analyzed for molecular measurements.

Terminal deoxynucleotidyl transferase dUTP nick end labeling (TUNEL) staining

Apoptosis was detected and quantified by the TUNEL assay using the In Situ Cell Death Detection Kit according to manufacturer protocols (Sigma-Aldrich). Five representative fields were selected from each group. The number of TUNEL positive cells in 500 cells was counted and AI was calculated. AI = apoptosis positive number/total number of cells·100%.

Quantitative real-time polymerase chain reaction (qRT-PCR)

Total RNA was extracted from cells or tissues using Trizol reagent (TaKaRa, Shiga, Japan). The RNA purity and concentration were determined according to the ratio 260/280 nm in a UV spectrophotometer. Total RNA was reverse transcribed into cDNA using the Revert Aid First Strand cDNA synthesis Kit (Thermo). qRT-PCR detection was subsequently performed using LightCyclerR 480 (Roche, Switzerland). The expression of Gapdh was used to normalize the gene expression levels. The primers of target genes were: IL-1β_F, CCGTGGACCTTCCAGGATGA; IL-1β_R, GGGAACGTCACACACCAGCA; IL-6_F, CTGCAAGAGACTTCCATCCAG; IL-6_R, AGTGGTATAGACAGGTCTGTTGG; TNF-α_F, CATCTTCTCAAAATTCGAGTGACAA; TNF-α_R, TGGGAGTAGACAAGGTACAACCC; MCP-1_F, TAAAAACCTGGATCGGAACCAAA; MCP-1_R, GCATTAGCTTCAGATTTACGGGT; GAPDH_F, ACCCTTAAGAGGGATGCTGC; GAPDH_R, CCCAATACGGCCAAATCCGT; Serinc2_F, GACTCTTTGTGTAACTGGCATC; Serinc2_R, AGCTTGTAAAGCTGACTCTCCA.

Western blot analysis

RIPA lysis buffer was used to extract protein from cells and frozen lung tissues. BCA protein quantitative kit was used to determine protein concentration. The same amount of protein (40 μg) in each sample was separated by SDS-PAGE and then transferred to PVDF membrane. After sealing these membranes with 5% skimmed milk powder at room temperature for 1 hour, these membranes were incubated overnight with the corresponding primary antibodies against SERINC2 (1:1000, PA5-49872, Invitrogen), p-STAT3 [1:1000, 9145, Cell Signaling Technology (CST)], STAT3 (1:1000, 12640, CST), p-p38 (1:1000, 4511, CST), p38 (1:1000, 8690, CST), p-ERK (1:1000, 4370S, CST), p44/42MPAK (ERK1/2; 1:1000, 9102S, CST), p-AKT (1:1000, 4060S, CST), AKT (1:000,9272S,CST), GAPDH (1:1000, 5174, CST) at 4 ℃. Then, it was incubated with the horseradish peroxidase binding second antibody at room temperature for 1 h. After that, the target strip was exposed on the chemiluminescence imaging system with chemiluminescence developer, and the target strip was quantitatively analyzed by Image J (National Institutes of Health). The GAPDH protein content in each sample was used as a reference.

Enzyme-linked immunosorbent assay (ELISA)

Mice was sacrificed 24h after CLP. the arterial blood was collected in heparin anticoagulant tube and centrifuged. The average absorbance value was determined by the corresponding enzyme-linked

immunosorbent assay (ELISA) kit, IL6 (Thermo Fisher, USA), TNFα (Thermo Fisher, USA). The absorbance of each well was recorded at 450nm using a microplate reader.

Bioinformatic analysis

Data files including GSE62107, GSE8608, GSE1871, GSE40885 and GSE45644 were downloaded from Gene Expression Omnibus (GEO) (http://www.ncbi.nlm.nih.gov/geo/). LPS stimulation used to perform ALI model in all these profiles. GSE62107 included 1 control sample and 1 LPS treatment sample, GSE8608 included 1 control sample and 1 LPS treatment sample, GSE1871 included 3 control sample and 3 LPS treatment sample, GSE40885 included 7 control sample and 7 LPS treatment sample, GSE45644 included 5 control sample and 5 LPS treatment sample.

Statistical analyses

Statistical analyses were performed using GraphPad Prism 8 Software. All experimental data are presented as mean ± SEM of at least three independent experiments. Statistical significance for multiple comparisons was determined by one-way ANOVA or two-way ANOVA followed by Tukey's test. Bonferroni adjustment was used for *post hoc* analysis. Student's *t* test was used for comparisons between two groups. $P < 0.05$ was considered statistically significant.

Results

Serinc2 deficiency exacerbates CLP-induced ALI

Since Serinc2 has been functionally involved in normal lung function [12, 13], we firstly explored the regulation of Serinc2 in ALI by examining its expression in available transcriptome profiles of ALI models. The expression level of Serinc2 was upregulated in 4 out of 5 GEO databases with LPS treatment (Fig. 1A). We then performed CLP surgery to induce ALI and found that both the mRNA (Fig. 1B) and the protein (Fig. 1C and 1D) expression of Serinc2 significantly increased in the lung after CLP surgery, suggesting a possible involvement of Serinc2 in the pathogenesis of CLP-induced ALI.

To investigate the physiological role of Serinc2, we generated a Serinc2-KO ($Serinc2^{-/-}$) mouse line using the CRISPR/Cas9 system (Fig. 1D). Heterozygous $serinc2^{+/-}$ mice had normal fertility and gave birth to $Serinc2^{+/+}$, $Serinc2^{+/-}$, and $Serinc2^{-/-}$ mice basically according to Mendel's law as expected (**Supplementary Table 1**). Mating between male and female $Serinc2^{-/-}$ mice also gave birth to normally developed $Serinc2^{-/-}$ mice (Fig. 1E and 1F), suggesting that Serinc2 is dispensable for gametogenesis and development.

When these mice were subjected to CLP surgery, however, three out of 10 $Serinc2^{-/-}$ mice died from CLP-induced sepsis within 24 hours, while all WT mice survived. Serinc2 deficiency significantly increased the CLP-induced EB dye leakage (Fig. 1G). Moreover, Serinc2 deficiency exacerbated ALI pathologies, including increased lung septum, pulmonary vascular congestion and inflammatory cell infiltration

(Fig. 1H). Consistently, histologic ALI scoring in Serinc2$^{-/-}$ mice was significantly elevated compared with WT after CLP (Fig. 1I). These data suggest that Serinc2 plays a protective role in CLP-induced ALI, while its upregulation in ALI might contribute as an endogenous protective feedback response.

Serinc2 KO promotes inflammatory responses and activates STAT3, p38 and ERK pathways in CLP-induced ALI

Cytokines such as IL1β,IL6, TNFα and MCP1 are involved in the inflammation process during ALI [3,4]. We measured the expression of these cytokines in the lung by qRT-PCR. The results showed that Serinc2 deficiency induced expression of IL1β, IL6, TNFα and MCP1 at basal condition, and further enhanced their increased mRNA levels after CLP (Fig. 2A). Consistently, ELISA assay detected significant increases in circulating IL6 and TNFα in the Serinc2-KO group compared with the WT controls both in sham and CLP groups (Fig. 2B), suggesting that Serinc2 deficiency augments the inflammatory responses in CLP-induced ALI.

Host inflammation responses in sepsis-associated ALI are mediated by pro-inflammatory signaling pathways, such as signal transducers and activators of transcription 3 (STAT3), extracellular signal-regulated kinase (ERK), p38, and etc [17–23]. Western blot analysis detected significant increases in phosphorylation of STAT3, p38 and ERK 24h after CLP in WT mice, which were further enhanced in Serinc2-KO mice (Fig. 2C and 2D), suggesting that the impact of Serinc2 deficiency on inflammation is mediated by the hyperactivation of these pro-inflammatory pathways.

Serinc2 overexpression ameliorates LPS-induced inflammation in RAW264.7 cells

Macrophage plays a central role in the initiation, maintenance and remission of inflammation during infection [24]. To determine the protective effect of Serinc2 in ALI, we overexpressed Serinc2 in LPS-stimulated RAW264.7 macrophages (Fig. 3A). At basal level, Serinc2 overexpression reduced the expression of IL1β, IL6, TNFα and MCP1 (Fig. 3B). LPS treatment (1μg/ml) for 24h induced the expression of IL1β, IL6, TNFα and MCP1, which were significantly reversed by Serinc2 overexpression (Fig. 3B). These data suggest that Serinc2 overexpression is powerful to suppress inflammation in ALI.

Phosphorylated STAT3 was time-dependently increased after LPS treatment in RAW264.7 cells, whereas ERK and p38 phosphorylations were immediately enhanced upon LPS treatment (0.5h) (Fig. 3C). After Serinc2 overexpression, the LPS-activated STAT3, p38 and ERK were significantly inhibited (Fig. 3D and 3E).

Serinc2 inhibits cell apoptosis in ALI

Cell death is a major manifestation of ALI, and plays a causal role in alveolar capillary barrier damage, fluid leakage and pulmonary hemorrhage [7–9]. We then examined the effect of Serinc2 KO on apoptosis by TUNEL staining of lung tissues with or without CLP surgery. The results showed that CLP significantly increased the number of TUNEL positive cells, which was further amplified in Serinc2 KO group (Fig. 4A).

Consistently, the increases in cleaved caspase-3 and Bax expression after CLP were enhanced by Serinc2 deficiency, while the reduced expression of Bcl2 was further diminished (Fig. 4B and 4C). AKT signaling pathway plays a pivotal role in cell survival [25, 26]. We observed that Akt phosphorylation was significantly activated by CLP, a pattern that was substantially reversed by Serinc2 KO (Fig. 4D and 4E). These data suggest that Serinc2 deficiency promotes apoptosis-associated cell death in ALI possibly dependent on Akt signaling pathway.

To test the anti-apoptosis function of Serinc2, we examined the apoptosis levels in LPS-treated RAW264.7 cells with or without Serinc2 overexpression. The results showed that Serinc2 overexpression significantly suppressed the LPS-induced increase in TUNEL positive cells (Fig. 5A), and reversed the LPS-induced changes in cleaved caspase-3, Bax and Bcl2 (Fig. 5B and 5C). Moreover, Serinc2 overexpression increased Akt phosphorylation at basal condition, and further enhanced it after LPS treatment (Fig. 5D and 5E). These results suggest a pro-survival role of Serinc2 in ALI.

Akt signaling pathway mediates the pro-survival role of Serinc2 in ALI

To validate that Akt signaling pathway mediating Serinc2's protective function in ALI, we employed an Akt-specific inhibitor AKTin [27–29]. Administration of AKTin (1μM) in RAW264.7 cells significantly blocked the inhibition of LPS-induced increase in TUNEL positive cells by Serinc2 overexpression (Fig. 6A). Consistently, the protective effects of Serinc2 overexpression on LPS-induced increases in cleaved caspase-3 and Bax and decrease in Bcl2 were substantially reversed by AKTin treatment (Fig. 6B and 6C). Moreover, AKTin largely abolished the inhibition of Serinc2 overexpression on inflammatory factors, albeit not achieving statistical significance for IL6, TNFa and MCP-1 (Fig. 6D). These data suggest that Akt signaling pathway contributes to Serinc2-mediated protection from apoptosis and inflammation.

Discussion

The pathogenesis of sepsis-associated ALI is manifested by inflammatory cascade and apoptosis accumulation. Our findings in this study identify Serinc2 as a novel protective regulator in the development of ALI pathologies both *in vitro* and *in vivo*. While the upregulation of Serinc2 during ALI might contribute as an endogenous protection feedback.

Serinc family is highly conserved in all eukaryotes and has similar transmembrane topology. This transmembrane topology has 10 transmembrane segments and contains a functional domain "helix-loop-helix" [30]. The Serinc family contains five members: Serinc1, Serinc2, Serinc3, Seinc4 and Serinc5. By integrating serine, a non-essential amino acid, into the cell membrane, its crucial function is to promote the production of phosphatidylserine and sphingomyelin, and regulate the biosynthesis of membrane lipid molecules [11]. Serinc5 has been proved to be the most powerful antiviral factor and can inhibit HIV, MLV, EIAV and so on [31]. It selectively inactivates envelope glycoprotein, interferes with the remaining env activity, prevents the folding of envelope, and then limits the infection of offspring virus to new target

cells [32]. In addition, serinc1 and serinc3 have also been observed to have limited HIV inhibition. Interestingly, serinc2, also known as tumor differentially expressed 2, has been firstly identified in non-small cell lung cancer cells [12], and has no effects on the infectivity of HIV-1 [32]. Here we, for the first time, reveal a protective role of Serinc2 in sepsis-associated ALI through inhibiting apoptosis and inflammation.

The plasma membrane is of great significance for the extracellular to intracellular transmembrane signal transduction of membrane receptors. Plasma membrane microcapsules and lipid rafts are lipid ordered domains rich in cholesterol and sphingomyelin, and enrich a variety of intracellular proteins involved in signal transduction [33]. Intact plasma membrane microcapsules and lipid rafts are important molecular basis for signal transduction, especially transmembrane signal transduction [33]. Emerging evidence reveals that the production of phosphatidylserine, “apoptosis clearance signaling”, inhibits leukocyte migration and promotes inflammation resolution [34]. As a cofactor, phosphatidylserine is required for the activation of TAM family, and further plays a counter-inflammation response in macrophages [35, 36]. The main function of Serinc2 is to assist in lipid synthesis on plasma membrane [11]. Our findings indicate that Serinc2 might contribute to the quench of the activated inflammation signaling, which depends on lipid raft integrity and mobility. As a key molecule in the synthesis of membrane lipids, whether Serinc2 also plays a protective role in ALI via the synthesis of phosphatidylserine and sphingomyelin needs to be investigated in future.

Production of inflammatory factors is mainly mediated by transcription factors, especially STAT3, which is responsible for transducing extracellular stimuli to nuclear gene expression through translocation from cytosol to nucleus after phosphorylation [37]. Persistent activation of STAT3 mediates both the release of proinflammatory cytokines and the suppression of anti-immune response in M1 pro-inflammatory macrophages [38–40]. This was further confirmed by our findings that the increasing phosphorylation lever of STAT3 according to time the of LPS challenge and the expression of p-STAT3 was downregulated while inflammatory response was alleviated.

As the center of signal transduction pathways, MAPK (mitogen-activated protein kinase, MAPK) pathway can be activated by various stimuli such as cytokines, radiation, osmotic pressure [17]. Activated MAPK receives signals that are converted and transmitted by membrane receptors and carries them into the nucleus, playing a pivotal role in cell proliferation and other biofunctions. ERK widely exists in various tissues, is involved in cell proliferation and differentiation. p38, mediating inflammation and apoptosis, many of whose specific inhibitor have shown early anti-inflammatory efficacy, even the p38γ inhibitor have been used in clinical treatment of idiopathic pulmonary fibrosis [22, 23, 41]. In the present study, we found that p38 and ERK were evoked by inflammatory stimuli including CLP and LPS, which could be modified by Serinc2. Considering the function of Serinc2 in membrane trafficking, our data implicate a crucial role of Serinc2-mediated membrane event in organizing transmembrane signaling transduction.

The activation of AKT mainly occurs on the cell membrane. When cells suffered from extracellular signals, activated PI3K generates PIP3 and transposes it to the cell membrane, which not only enables AKT itself to obtain catalytic activity, but also enables Both AKT and PDK-1 to be co-located on the cell membrane. PDK-1 can further catalyse AKT phosphorylation and make it fully activated, thereby regulating the phenotypes of cell proliferation, differentiation, apoptosis and migration [28, 42]. Corresponding to in vivo experiments, we used an inflammatory response model of ALI induced by LPS. It was confirmed that up-regulation of serinc2 can lead to a decrease the apoptosis associated protein and reduced of TUNEL cells. Furthermore, our *in vitro* analyses further verify that serinc2 could inhibits apoptosis by activation of Akt, as evidenced by negligible changes in LPS-induced effects, containing elevated cleaved-caspase3, Bax and decreased Bcl2 protein expression, along with increases in TUNEL cells after AKTin pre-treatment. Additionally, previous studies demonstrating activation of PI3K/Akt signaling pathway suppresses the LPS-induced inflammatory caspases in ALI [43, 44]. In the present study, we found the inhibitor of Akt blocked the protective effect of serinc2 against inflammation in ALI, implying that serinc2 prevents LPS-induced inflammation and apoptosis partially by the Akt pathway. However, it is unclear whether the special membrane trafficking function of serinc2 can activate Akt or there is a spatial interaction between serinc2 and Akt, which needs further experimental proof.

COVID-19 pandemic and its subsequent development into ALI/ARDS threaten the lives of millions of people worldwide, and the adverse progress of COVID-19 is related to the severe inflammatory response and cell injury by virus infection [45, 46]. COVID-19, as a specific intracellular parasitic pathogen, from the initial adsorption, penetration into host cells to the final release of progeny cells, is inseparable from the cell membrane of host cells. As an important regulator of membrane lipid synthesis, serinc2 can not only regulate inflammatory signal pathway, promote cell survival and inhibit cell apoptosis, but also can be a promising candidate in the development of new anti-COVID-19 approaches and may be an effective target to treat COVID-19 clinical complications.

Conclusion

Taken together, our data demonstrate that Serinc2 functions as an endogenous protector against sepsis-associated ALI through suppression of STAT3, p38 and ERK pathways and activation of the Akt pathway. Our findings provide novel insights into the pathogenesis of sepsis-associated ALI, and reveal potential strategies to treat ALI in clinic.

Abbreviations

AKT, protein kinase B

ALI, acute lung injury

ARDS, acute respiratory distress syndrome

CLP, cecal ligation and puncture

CXCL2, CXC chemokine ligands 2

EB, Evans blue

EIAV, Equine infectious anemia virus

ELISA, enzyme-linked immunosorbent assay

ERK, extracellular signal-regulated kinase

GEO, Gene Expression Omnibus

H&E, Hematoxylin and Eosin

HIV, human immunodeficiency virus

IL1, interleukin-1

IL6, interleukin-6

KO, knockout

LPS , lipopolysaccharide

MAPK, mitogen-activated protein kinase

MCP-1, monocyte chemoattractant protein-1

MLV, Murine Leukemia Virus

Serinc2, serine incorporator 2

STAT3, signal transducers and activators of transcription 3

TNFα, tumor necrosis factor α

TUNEL, terminal deoxynucleotidyl transferase dUTP nick end labeling

Declarations

Acknowledgements

Not applied.

Author Contributions

ZW, GW and XH conceived and supervised the project. SM performed the cell and molecular experiments with inputs from NG, YF and JT. JL and MC performed the CLP surgery. SM and ZW analyzed the data and drafted the manuscript. All authors have access to the original data and approved the publication of the manuscript.

Funding

This study was supported by funds from National Natural Science Foundation of China (nos. 81722007, 82070231 and 81870301), National Health Commission of China (no. 2017ZX1030440 2001-008), State Key Laboratory of Cardiovascular Disease (nos. GZ2021015, 2021-YJR01 and SKL2021022), and start-up funds from Fuwai Hospital Chinese Academy of Medical Sciences, Shenzhen (GSP-RC-2020002).

Data availability

All data generated or analyzed during this study are included in the manuscript. GEO databases are available online (https://www.ncbi.nlm.nih.gov/).

Ethics Statement

All animal experiments procedures were reviewed and approved by the Institutional Animal Care and Use Committee (IACUC) of Renmin Hospital of Wuhan University and performed in accordance with the guide for the care and use of laboratory animals published by National Institutes of Health, USA (8th edition).

Competing interests

The authors declare no competing interests.

References

1. Fan E, Brodie D, Slutsky AS. Acute Respiratory Distress Syndrome: Advances in Diagnosis and Treatment. JAMA. 2018;319:698–710.
2. Mowery NT, Terzian WTH, Nelson AC. Acute lung injury. Curr Probl Surg. 2020;57:100777.
3. Goodman RB, Pugin J, Lee JS, Matthay MA. Cytokine-mediated inflammation in acute lung injury. Cytokine Growth Factor Rev. 2003;14:523–35.
4. Navarro-Gonzalez JF, Mora-Fernandez C, Muros de Fuentes M, Garcia-Perez J. Inflammatory molecules and pathways in the pathogenesis of diabetic nephropathy. Nat Rev Nephrol. 2011;7:327–40.
5. Tian R, Wang X, Pan T, Li R, Wang J, Liu Z, Chen E, Mao E, Tan R, Chen Y, Liu J, Qu H. Plasma PTX3, MCP1 and Ang2 are early biomarkers to evaluate the severity of sepsis and septic shock. Scand J Immunol. 2019;90:e12823.
6. Hu Q, Lyon CJ, Fletcher JK, Tang W, Wan M, Hu TY. Extracellular vesicle activities regulating macrophage- and tissue-mediated injury and repair responses. Acta Pharm Sin B. 2021;11:1493–

512.

7. Chopra M, Reuben JS, Sharma AC. Acute lung injury:apoptosis and signaling mechanisms. Exp Biol Med (Maywood). 2009;234:361–71.
8. Karki R, Sharma BR, Tuladhar S, Williams EP, Zalduondo L, Samir P, Zheng M, Sundaram B, Banoth B, Malireddi RKS, Schreiner P, Neale G, Vogel P, Webby R, Jonsson CB, Kanneganti TD. Synergism of TNF-alpha and IFN-gamma Triggers Inflammatory Cell Death, Tissue Damage, and Mortality in SARS-CoV-2 Infection and Cytokine Shock Syndromes. Cell. 2021;184:149–68. e17.
9. Hotchkiss RS, Dunne WM, Swanson PE, Davis CG, Tinsley KW, Chang KC, Buchman TG, Karl IE. Role of apoptosis in Pseudomonas aeruginosa pneumonia. Science. 2001;294:1783.
10. Perl M, Chung CS, Perl U, Lomas-Neira J, de Paepe M, Cioffi WG, Ayala A. Fas-induced pulmonary apoptosis and inflammation during indirect acute lung injury. Am J Respir Crit Care Med. 2007;176:591–601.
11. Inuzuka M, Hayakawa M, Ingi T. Serinc, an activity-regulated protein family, incorporates serine into membrane lipid synthesis. J Biol Chem. 2005;280:35776–83.
12. Player A, Gillespie J, Fujii T, Fukuoka J, Dracheva T, Meerzaman D, Hong KM, Curran J, Attoh G, Travis W, Jen J. Identification ofTDE2 gene and its expression in non-small cell lung cancer. Int J Cancer. 2003;107:238–43.
13. Zeng Y, Xiao D, He H, He J, Pan H, Yang W, Chen Y, He J. SERINC2-knockdown inhibits proliferation, migration and invasion in lung adenocarcinoma. Oncol Lett. 2018;16:5916–22.
14. Bouchon A, Facchetti F, Weigand MA, Colonna M. TREM-1 amplifies inflammation and is a crucial mediator of septic shock. Nature. 2001;410:1103–7.
15. Matute-Bello G, Downey G, Moore BB, Groshong SD, Matthay MA, Slutsky AS, Kuebler WM. Acute Lung Injury in Animals Study G: An official American Thoracic Society workshop report: features and measurements of experimental acute lung injury in animals. Am J Respir Cell Mol Biol. 2011;44:725–38.
16. Artham S, Gao F, Verma A, Alwhaibi A, Sabbineni H, Hafez S, Ergul A, Somanath PR. Endothelial stromelysin1 regulation by the forkhead box-O transcription factors is crucial in the exudative phase of acute lung injury. Pharmacol Res. 2019;141:249–63.
17. Burton JC, Antoniades W, Okalova J, Roos MM, Grimsey NJ. Atypical p38 Signaling, Activation, and Implications for Disease. Int J Mol Sci 2021, 22.
18. Arthur JS, Ley SC. Mitogen-activated protein kinases in innate immunity. Nat Rev Immunol. 2013;13:679–92.
19. Yu H, Pardoll D, Jove R. STATs in cancer inflammation and immunity: a leading role for STAT3. Nat Rev Cancer. 2009;9:798–809.
20. Levy DE, Darnell JE Jr. Stats: transcriptional control and biological impact. Nat Rev Mol Cell Biol. 2002;3:651–62.

21. Nailwal NP, Doshi GM. Role of intracellular signaling pathways and their inhibitors in the treatment of inflammation. Inflammopharmacology. 2021;29:617–40.
22. Grimes JM, Grimes KV. p38 MAPK inhibition: A promising therapeutic approach for COVID-19. J Mol Cell Cardiol. 2020;144:63–5.
23. Schindler JF, Monahan JB, Smith WG. p38 pathway kinases as anti-inflammatory drug targets. J Dent Res. 2007;86:800–11.
24. Grivennikov SI, Greten FR, Karin M. Immunity, inflammation, and cancer. Cell. 2010;140:883–99.
25. Chien TM, Wu KH, Chuang YT, Yeh YC, Wang HR, Yeh BW, Yen CH, Yu TJ, Wu WJ, Chang HW. Withaferin A Triggers Apoptosis and DNA Damage in Bladder Cancer J82 Cells through Oxidative Stress. Antioxidants (Basel) 2021, 10.
26. Chen H, Wei L, Luo M, Wang X, Zhu C, Huang H, Liu X, Lu H, Zhong Y. LINC00324 suppresses apoptosis and autophagy in nasopharyngeal carcinoma through upregulation of PAD4 and activation of the PI3K/AKT signaling pathway. Cell Biology and Toxicology; 2021.
27. Wan Q, Yang M, Liu Z, Wu J. Ambient fine particulate matter aggravates atherosclerosis in apolipoprotein E knockout mice by iron overload via the hepcidin-ferroportin axis. Life Sci. 2021;264:118715.
28. Fan YL, Li HC, Zhao W, Peng HH, Huang F, Jiang WH, Xu SY. Curcumin Attenuated Bupivacaine-Induced Neurotoxicity in SH-SY5Y Cells Via Activation of the Akt Signaling Pathway. Neurochem Res. 2016;41:2425–32.
29. Jiang Y, Kou J, Han X, Li X, Zhong Z, Liu Z, Zheng Y, Tian Y, Yang L. ROS-Dependent Activation of Autophagy through the PI3K/Akt/mTOR Pathway Is Induced by Hydroxysafflor Yellow A-Sonodynamic Therapy in THP-1 Macrophages. Oxid Med Cell Longev. 2017;2017:8519169.
30. Pye VE, Rosa A, Bertelli C, Struwe WB, Maslen SL, Corey R, Liko I, Hassall M, Mattiuzzo G, Ballandras-Colas A, Nans A, Takeuchi Y, Stansfeld PJ, Skehel JM, Robinson CV, Pizzato M, Cherepanov P. A bipartite structural organization defines the SERINC family of HIV-1 restriction factors. Nat Struct Mol Biol. 2020;27:78–83.
31. Timilsina U, Umthong S, Lynch B, Stablewski A, Stavrou S: SERINC5 Potently Restricts Retrovirus Infection In Vivo. mBio 2020, 11.
32. Rosa A, Chande A, Ziglio S, De Sanctis V, Bertorelli R, Goh SL, McCauley SM, Nowosielska A, Antonarakis SE, Luban J, Santoni FA, Pizzato M. HIV-1 Nef promotes infection by excluding SERINC5 from virion incorporation. Nature. 2015;526:212–7.
33. Simons K, Toomre D. Lipid rafts and signal transduction. Nat Rev Mol Cell Biol. 2000;1:31–9.
34. Sordi R, Bet AC, Della Justina AM, Ramos GC, Assreuy J. The apoptosis clearance signal phosphatidylserine inhibits leukocyte migration and promotes inflammation resolution in vivo. Eur J Pharmacol. 2020;877:173095.
35. Burstyn-Cohen T, Maimon A. TAM receptors, Phosphatidylserine, inflammation, and Cancer. Cell Commun Signal. 2019;17:156.

36. Lumbroso D, Soboh S, Maimon A, Schif-Zuck S, Ariel A, Burstyn-Cohen T. Macrophage-Derived Protein S Facilitates Apoptotic Polymorphonuclear Cell Clearance by Resolution Phase Macrophages and Supports Their Reprogramming. Front Immunol. 2018;9:358.
37. Larsen SB, Cowley CJ, Sajjath SM, Barrows D, Yang Y, Carroll TS, Fuchs E. Establishment, maintenance, and recall of inflammatory memory. Cell Stem Cell 2021.
38. Kujawski M, Kortylewski M, Lee H, Herrmann A, Kay H, Yu H. Stat3 mediates myeloid cell-dependent tumor angiogenesis in mice. J Clin Invest. 2008;118:3367–77.
39. Qu X, Zhuang G, Yu L, Meng G, Ferrara N. Induction of Bv8 expression by granulocyte colony-stimulating factor in CD11b + Gr1 + cells: key role of Stat3 signaling. J Biol Chem. 2012;287:19574–84.
40. Yu H, Kortylewski M, Pardoll D. Crosstalk between cancer and immune cells: role of STAT3 in the tumour microenvironment. Nat Rev Immunol. 2007;7:41–51.
41. Cheriyan J, Webb AJ, Sarov-Blat L, Elkhawad M, Wallace SM, Maki-Petaja KM, Collier DJ, Morgan J, Fang Z, Willette RN, Lepore JJ, Cockcroft JR, Sprecher DL, Wilkinson IB. Inhibition of p38 mitogen-activated protein kinase improves nitric oxide-mediated vasodilatation and reduces inflammation in hypercholesterolemia. Circulation. 2011;123:515–23.
42. Riscal R, Bull CJ, Mesaros C, Finan JM, Carens M, Ho ES, Xu JP, Godfrey J, Brennan P, Johansson M, Purdue MP, Chanock SJ, Mariosa D, Timpson NJ, Vincent EE, Keith B, Blair IA, Skuli N, Simon MC: Cholesterol auxotrophy as a targetable vulnerability in clear cell renal cell carcinoma. Cancer Discovery 2021:candisc.0211.2021.
43. Luo X, Lin B, Gao Y, Lei X, Wang X, Li Y, Li T. Genipin attenuates mitochondrial-dependent apoptosis, endoplasmic reticulum stress, and inflammation via the PI3K/AKT pathway in acute lung injury. Int Immunopharmacol. 2019;76:105842.
44. Wan Q, Yang M, Liu Z, Wu J. Atmospheric fine particulate matter exposure exacerbates atherosclerosis in apolipoprotein E knockout mice by inhibiting autophagy in macrophages via the PI3K/Akt/mTOR signaling pathway. Ecotoxicol Environ Saf. 2021;208:111440.
45. Connors JM, Levy JH. COVID-19 and its implications for thrombosis and anticoagulation. Blood. 2020;135:2033–40.
46. Xu Z, Shi L, Wang Y, Zhang J, Huang L, Zhang C, Liu S, Zhao P, Liu H, Zhu L, Tai Y, Bai C, Gao T, Song J, Xia P, Dong J, Zhao J, Wang F-S. Pathological findings of COVID-19 associated with acute respiratory distress syndrome. The Lancet Respiratory Medicine. 2020;8:420–2.

Figures

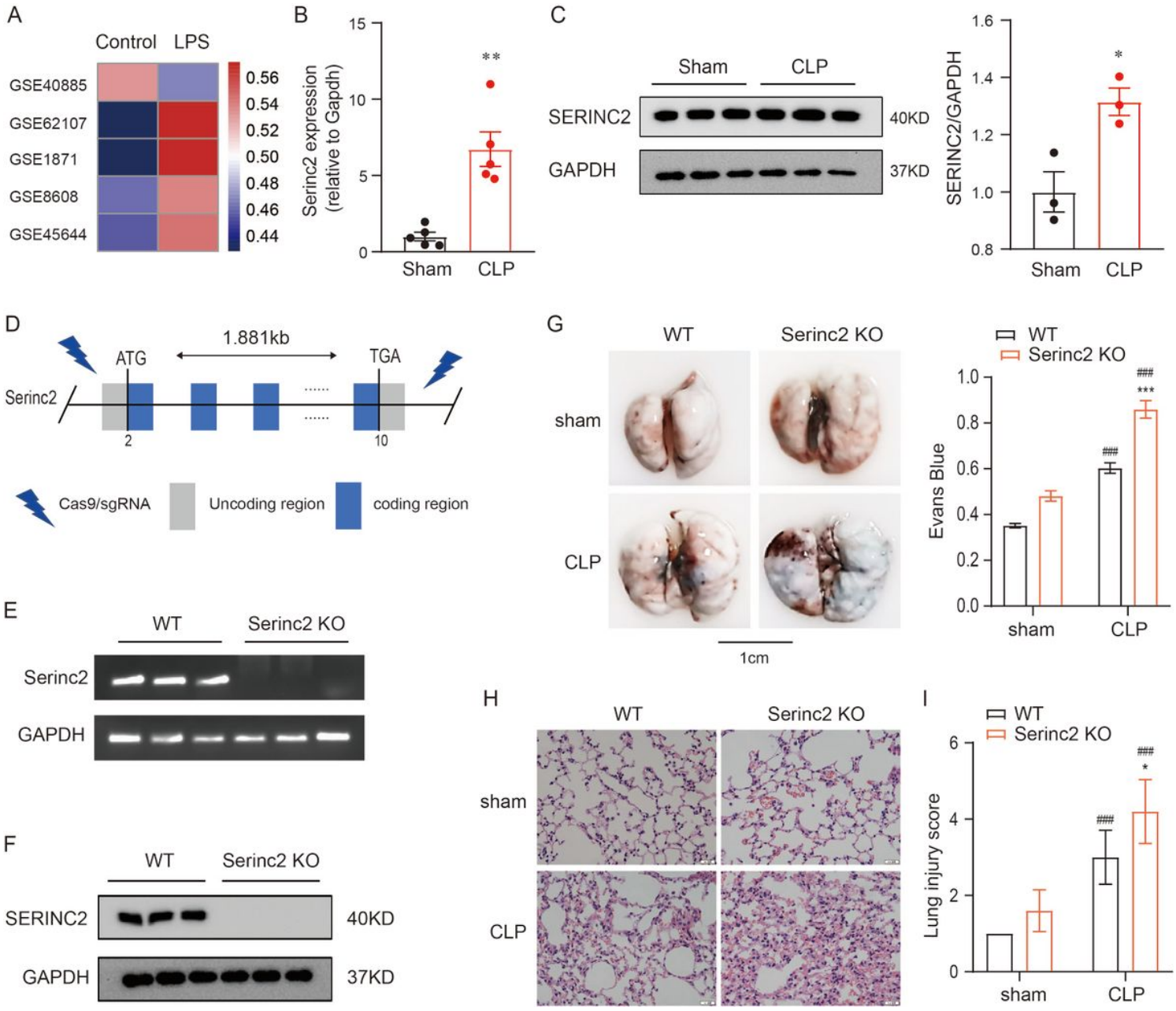

Figure 1

Serinc2 KO exacerbates CLP-induced ALI. A. Bioinformatic analysis showing the regulation of Serinc2 expression after LPS stimulation from indicated GEO databases. B. Effect of CLP on Serinc2 expression at the mRNA level in the lung measured by qRT-PCR. **p<0.01 vs. sham; n = 5. C. Immunoblots (left) and Quantification data (right) showing the expression of SERINC2 in the lung tissues of mice with sham or CLP surgeries. GADPH serves as the inner control. *p<0.05 versus CLP alone. *p<0.05 vs. sham; n = 5. D. Schematic showing the strategy to generate Serinc2 knockout (Serinc2-/-) mouse using CRISPR/Cas9 technology. E. Validation of Serinc2 knockout by agarose gel electrophoresis for the PCR products with Serinc2 (Exon2-10) primers. F. Immunoblots showing the complete knockout of SERINC2 in the lung tissues. G. Representative Evan's blue images (left) and quantification data (right) showing the impact of Serinc2 knockout on alveolar capillary barrier damage induced by CLP. ***P < 0.001 vs. WT; ###P < 0.001 vs. sham. n = 5. H. Representative H&E staining images showing the impact of Serinc2 knockout on CLP-

induced pathology. n = 5. I. ALI scoring for the H&E staining images as described in Methods. *P < 0.05 vs. WT group; ###P < 0.001 vs. sham. n = 5.

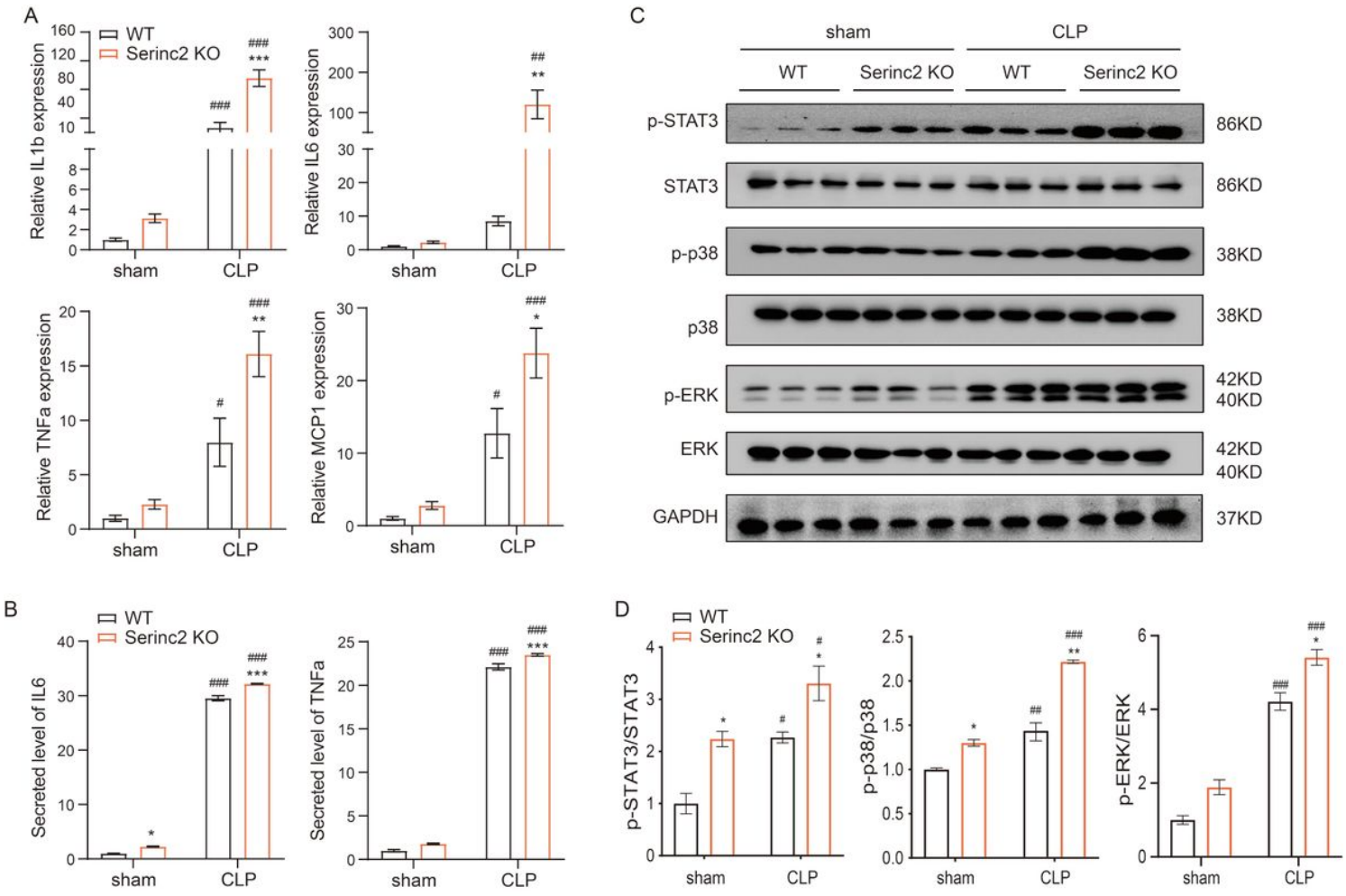

Figure 2

Serinc2 KO enhances CLP-induced hyperactivation of inflammation. A. Impact of Serinc2 KO on CLP-induced expression of IL1β, IL6, TNFα, and MCP1 measured by qRT-PCR. *P < 0.05, **P < 0.01, ***P < 0.001 vs. WT; #P < 0.05, ##P < 0.01, ###P < 0.001 vs. sham. n = 5-7. B. Impact of Serinc2 KO on CLP-induced secretion of IL6 and TNFα in serum assessed by ELISA kits. *P < 0.05, ***P < 0.001 vs. WT; ###P < 0.001 vs. sham. n = 5-7. C. Immunoblots of phosphorylated and total STAT3, p38 and ERK in the lung tissues from WT and Serinc2-KO mice with sham or CLP surgeries. D. Quantification of STAT3, p38 and ERK phosphorylation levels in ratio to their total protein. *P < 0.05, **P < 0.01 vs. WT; #P < 0.05, ##P < 0.01, ###P < 0.001 vs. sham. n = 3.

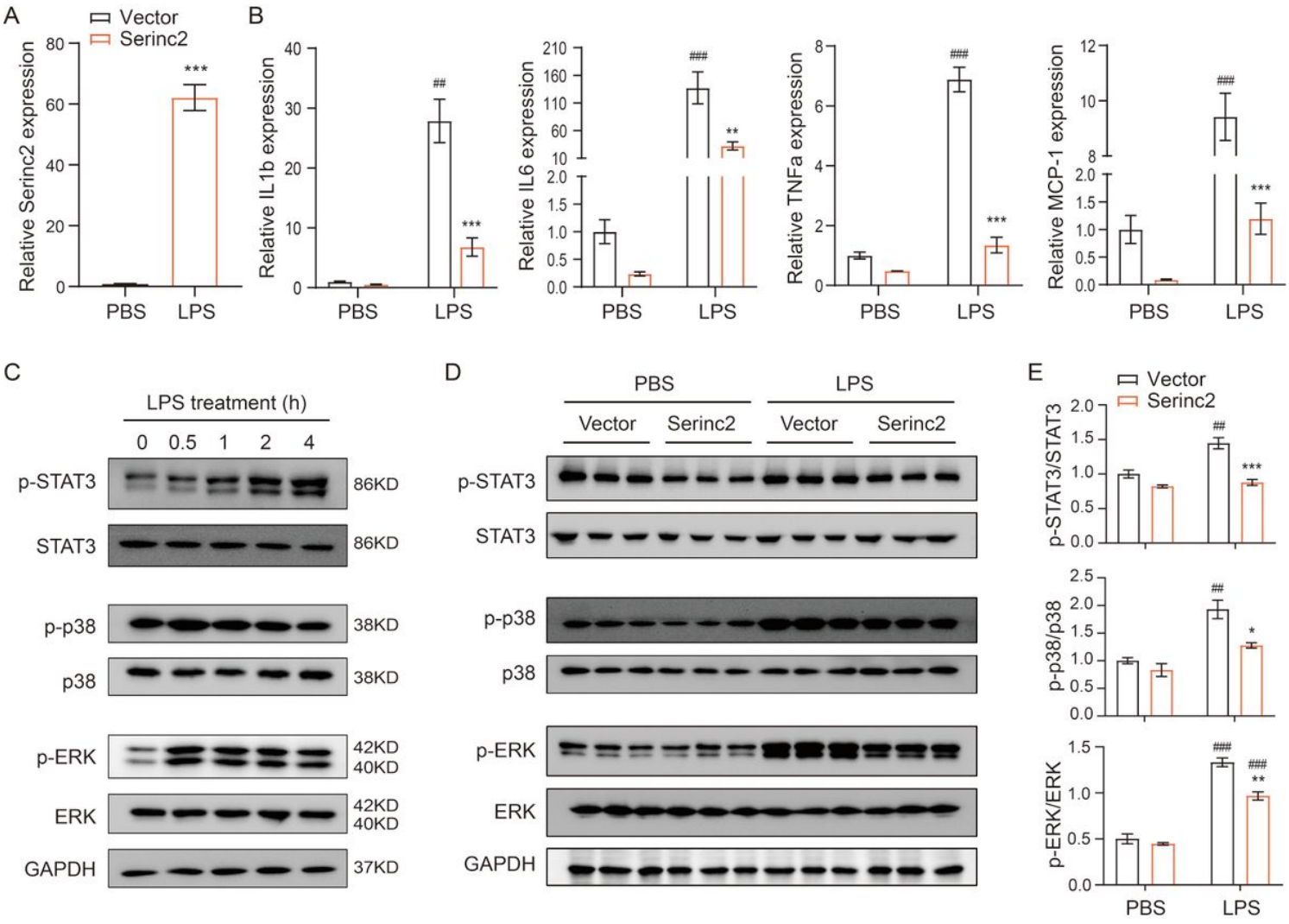

Figure 3

Serinc2 overexpression protects RAW264.7 cells from LPS-induced inflammation. A. Validation of Serinc2 overexpression by qRT-PCR. RAW264.7 cells were transfected with Vector or Serinc2 plasmid (4μg) for 48h. ***P < 0.001 vs. Vector. n = 3. B. Effects of Serinc2 overexpression on LPS-induced expression of IL1β, IL6, TNFα, and MCP1 in RAW264.7 cells. LPS (1μg) was administrated for 4h. **P < 0.01, ***P < 0.001 vs. Vector; ##P < 0.01, ###P < 0.001 vs. PBS. n = 3. C. Time-dependent activation of STAT3, p38 and ERK pathways by LPS in RAW264.7 cells measured by Western blot. D. Immuoblots showing the impact of Serinc2 overexpression on LPS-induced phosphorylation of STAT3, p38 and ERK. E. Quantification of STAT3, p38 and ERK phosphorylation levels in ratio to their total protein. *P < 0.05, **P < 0.01, ***P < 0.001 vs. Vector; ##P < 0.01, ###P < 0.001 vs. PBS. n = 3.

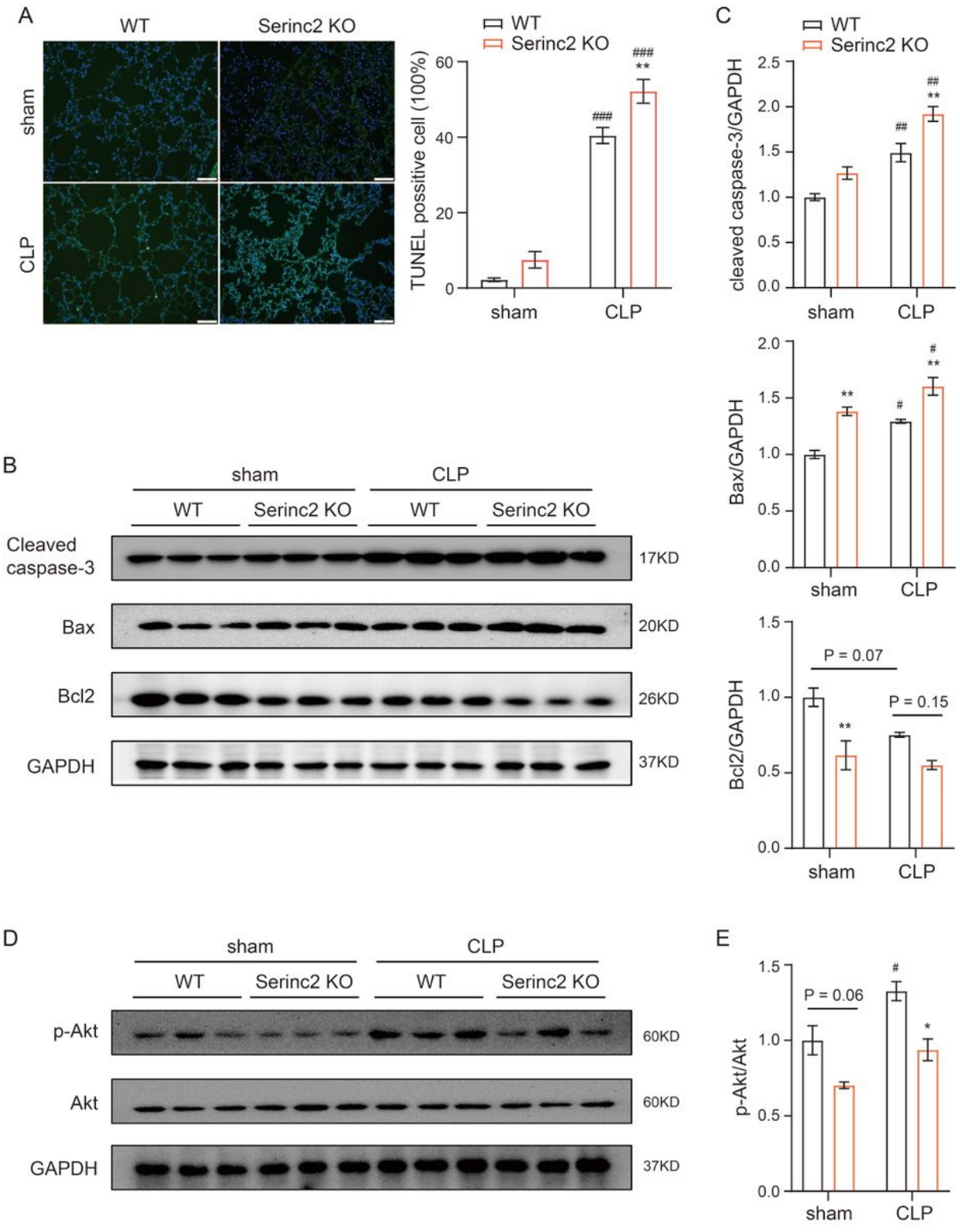

Figure 4

Serinc2 KO aggravates CLP-induced apoptosis in the lung. A. Representative TUNEL staining images (left) and quantification data (right) showing the impact of Serinc2 KO on CLP-induced apoptosis. **P < 0.01 vs. WT; ###P < 0.001 vs. sham. n = 5. B. Immunoblots showing the impact of Serinc2 KO on CLP-induced changes of cleaved caspase-3, Bax and Bcl2. C. Quantification of cleaved caspase-3, Bax and Bcl2 expression relative to GAPDH. **P < 0.01 vs. WT; #P < 0.05, ##P < 0.01 vs. sham. n = 3. D.

Immunoblots showing the impact of Serinc2 KO on CLP-induced Akt phosphorylation. E. Quantification of Akt phosphorylation relative to its total protein. *P < 0.05 vs. WT; #P < 0.05 vs. sham. n = 3.

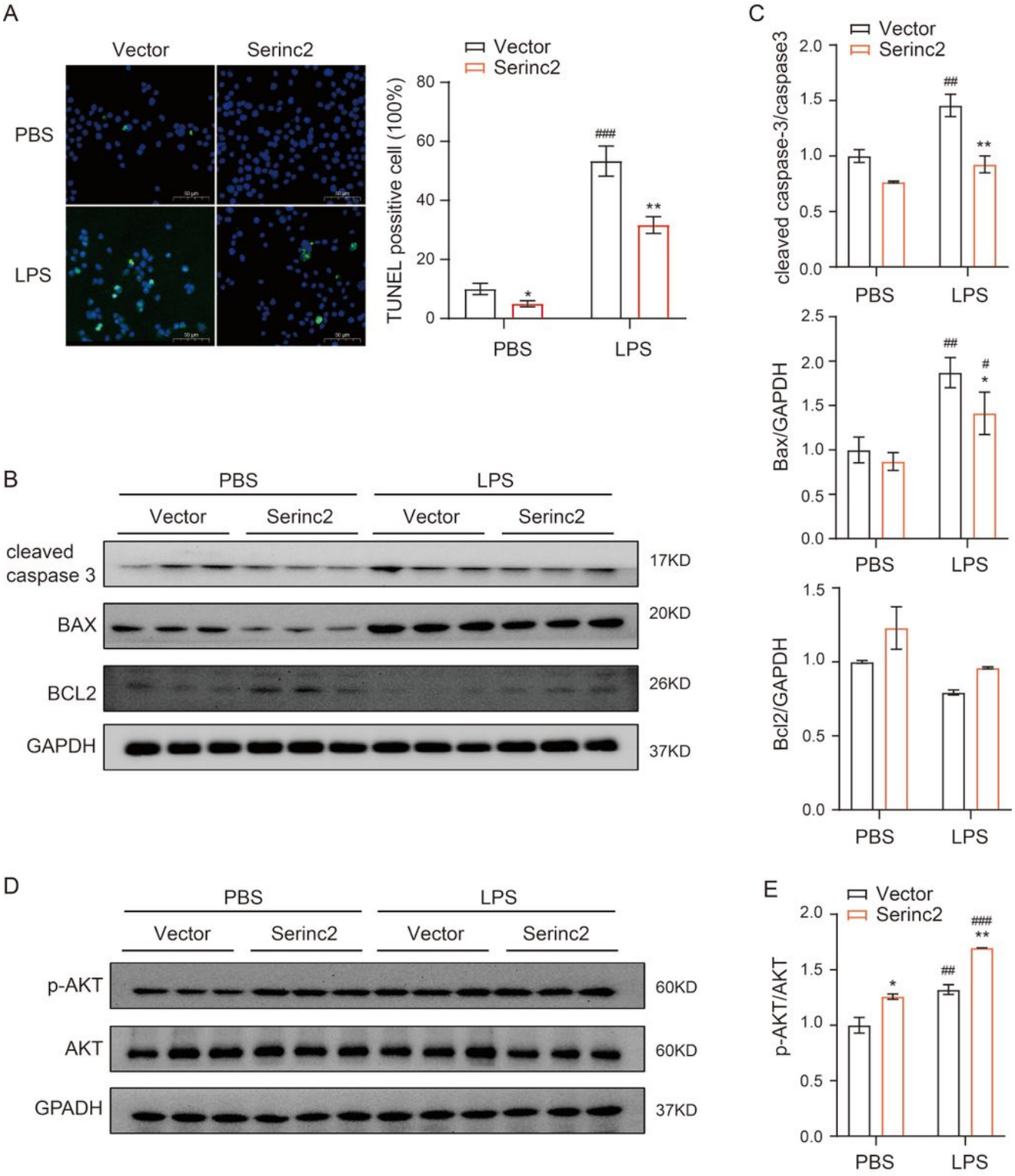

Figure 5

Serinc2 overexpression inhibits LPS-induced apoptosis in RAW264.7 cells. A. Representative TUNEL staining images (left) and quantification data (right) showing the impact of Serinc2 overexpression on LPS-induced apoptosis in RAW264.7 cells. *P < 0.05, **P < 0.01 vs. Vector; ##P < 0.01 vs. PBS. n = 3. B.

Immunoblots showing the impact of Serinc2 overexpression on LPS-induced changes of cleaved caspase-3, Bax and Bcl2. C. Quantification of cleaved caspase-3, Bax and Bcl2 expression relative to GAPDH. *P < 0.05, **P < 0.01 vs. Vector; #P < 0.05, ##P < 0.01 vs. PBS. n = 3. D. Immunoblots showing the impact of Serinc2 overexpression on LPS-induced Akt phosphorylation. E. Quantification of Akt phosphorylation relative to its total protein. *P < 0.05, **P < 0.01 vs. Vector; ##P < 0.01, ###P < 0.001 vs. PBS. n = 3.

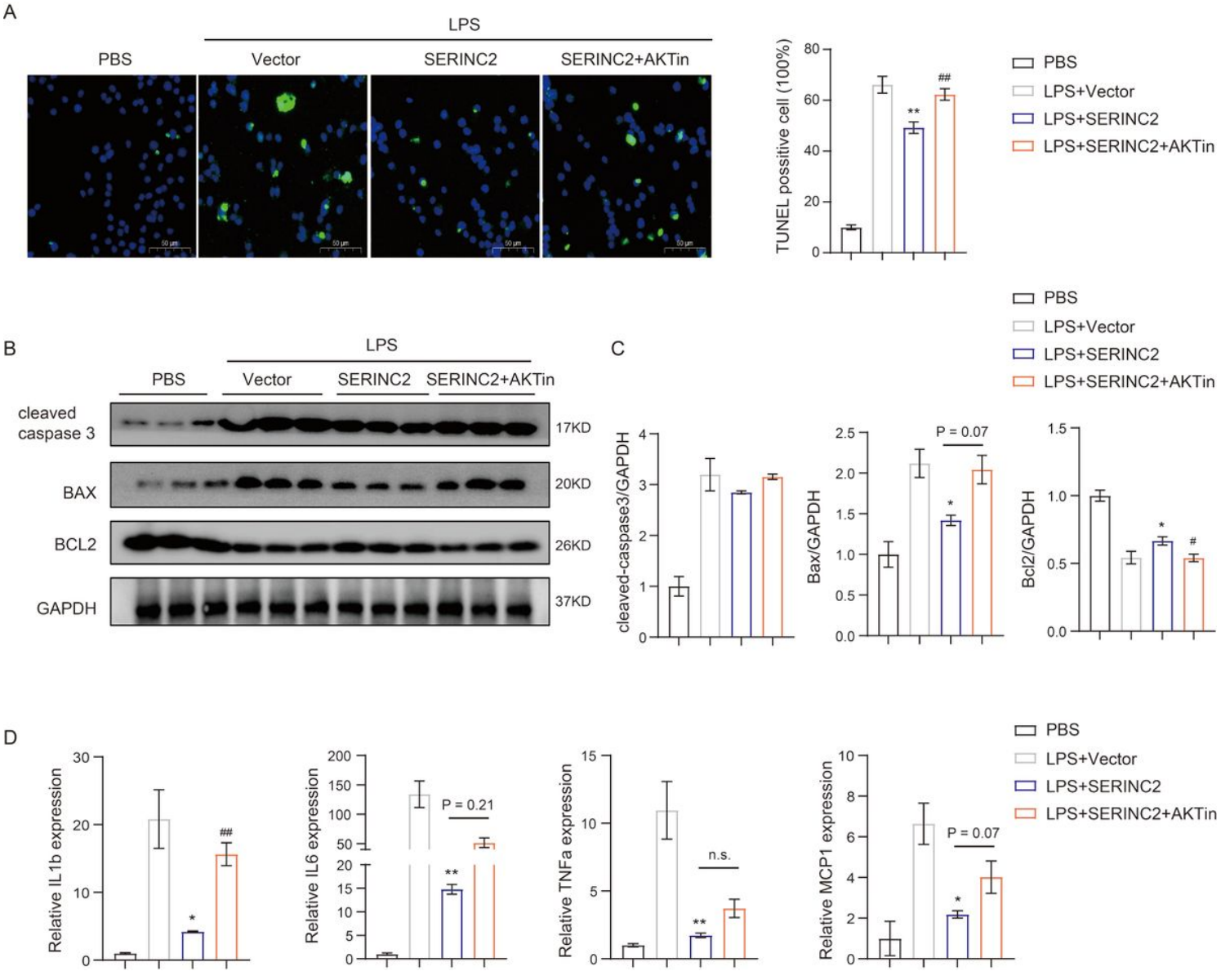

Figure 6

Akt pathway mediates the protective effects of Serinc2 in LPS-treated RAW264.7 cells. A. Representative TUNEL staining images (left) and quantification data (right) in PBS, LPS+vector, LPS+Serinc2, and LPS+Serinc2+AKTin groups. AKTin (1μM) was administrated to RAW264.7 cells for 24h. **P < 0.01 vs. LPS+Vector; ##P < 0.01 vs. LPS+Serinc2. n = 3. B. Immunoblots of cleaved caspase-3, Bax and Bcl2 in PBS, LPS+vector, LPS+Serinc2, and LPS+Serinc2+AKTin groups. C. Quantification of cleaved caspase-3, Bax and Bcl2 expression relative to GAPDH. *P < 0.05 vs. LPS+Vector; #P < 0.05, ##P < 0.01 vs.

LPS+Serinc2. n = 3. D. Expression of IL1β, IL6, TNFα, and MCP1 in PBS, LPS+vector, LPS+Serinc2, and LPS+Serinc2+AKTin groups detected by qRT-PCR. *P < 0.05, **P < 0.01 vs. LPS+Vector; ##P < 0.01 vs. LPS+Serinc2. n = 3.

Supplementary Files

This is a list of supplementary files associated with this preprint. Click to download.

- SupplementaryTable1.docx